Investigation of the host and environmental-associated microbiome to the mercury detoxification strategies of two Caiman species in French Guiana.

Mason H. Scarpa

Department of Behavioral and Cognitive Biology, Djerassiplatz 1, 1130 Vienna, Austria
(scarpa.mason@gmail.com)

Abstract. Mercury (Hg) contamination presents a critical threat to wildlife in regions affected by artisanal and small-scale gold mining. Neotropical caimans, as long-lived apex predators, are particularly exposed to mercury bioaccumulation, yet microbial mechanisms that may influence mercury detoxification remain insufficiently understood. This study investigated the taxonomic structure and potential microbial contributions to mercury detoxification in host-associated (cloaca, skin) and environmental (soil) microbiomes of *Melanosuchus niger* and *Paleosuchus trigonatus* across a natural Hg gradient in French Guiana. Using 16S rRNA amplicon sequencing and nested PCR screening for the *merA* gene, we characterized microbial communities and evaluated multivariate responses to mercury exposure. Microbiomes were primarily structured by environmental compartment and spatial context, with host species identity contributing to variation within each compartment. Multivariate analyses indicated that mercury significantly contributed to soil community composition independently of geography, whereas skin and cloacal microbiomes showed no significant mercury-associated structuring. Alpha diversity did not differ significantly between low- and high-mercury groups, although trends suggested reduced diversity in cloacal communities and increased richness in skin communities under higher Hg. *merA* was detected in all compartments but showed no quantitative relationship with Hg levels. Soil microbial co-occurrence networks contracted under high Hg, whereas host-associated networks remained stable. Collectively, these results indicate that host-associated microbiomes are comparatively robust to mercury exposure, while soil microbiomes provide more sensitive indicators of environmental Hg stress, underscoring the importance of environmental context in shaping microbial responses to contamination in Neotropical caimans.

Introduction. Mercury is a global contaminant originating from both natural and anthropogenic sources (Driscoll et al., 2013; Chen et al., 2018). In French Guiana, artisanal small-scale gold mining (ASGM) is the dominant source of Hg release, driving contamination of terrestrial and aquatic ecosystems (Esdaile and Chalker, 2018; AMAP, 2021; Scammacca et al., 2021). As Hg bioaccumulates and biomagnifies through food webs, apex predators such as caimans experience some of the highest exposure levels (Eagles-Smith et al., 2018; Lemaire et al., 2021a; Lemaire et al., 2024). Elevated Hg concentrations in caimans have been associated with impaired osmoregulation, hepatic dysfunction, endocrine disruption, altered blood chemistry, and maternal transfer to offspring (Lemaire et al., 2021a; Lemaire et al., 2021b; Lemaire et al., 2022).

The Black caiman (*Melanosuchus niger*) and the Smooth-fronted caiman (*Paleosuchus trigonatus*) occupy distinct ecological niches: *M. niger* is primarily aquatic and exposed to aquatic Hg sources, whereas *P. trigonatus* uses semi-terrestrial habitats with differing trophic pathways and selenium intake (Caut et al., 2019; Lemaire et al., 2021a; Lemaire et al., 2022). These ecological differences result in contrasting Hg burdens and selenium co-exposure patterns, reflected in markedly different Se:Hg molar ratios between species (Lemaire et al., 2021a; Lemaire et al., 2022). Such interspecific variation suggests species-specific detoxification constraints or requirements. To date, research has largely focused on

physiological and trophic determinants of Hg exposure in caimans, leaving microbial contributions unexplored (Lemaire, 2023).

Microorganisms influence Hg speciation by participating in methylation, demethylation, and reduction of inorganic Hg (Barkay et al., 2003; Barkay and Gu, 2021). Mercury-resistant bacteria (MRB) carry the *mer* operon, enabling enzymatic reduction of Hg^{2+} to volatile Hg^0 (Nascimento and Chartone-Souza, 2003; Barkay et al., 2003; Mathema et al., 2011). The key enzyme, MerA, catalyzes this reaction and is widespread across bacterial taxa, including Proteobacteria, Actinobacteriota, Firmicutes, and Bacteroidota (Christakis et al., 2021). In mercury-contaminated environments, microbial communities undergo compositional and functional restructuring, often characterized by enrichment of resistant taxa and shifts in diversity and network structure (Müller et al., 2001; Müller et al., 2001b; Frey and Rieder, 2013; Frossard et al., 2018).

Despite extensive evidence for microbial Hg transformation in soils and aquatic systems, the role of MRB within host-associated microbiomes of wildlife remains poorly characterized. This knowledge gap is particularly relevant for caimans, which are increasingly used as bioindicators of Hg contamination in tropical ecosystems (Lemaire, 2023). Understanding whether host-associated microbiomes contribute to Hg detoxification or tolerance is therefore essential for interpreting Hg burdens in caimans and for refining their application as sentinels of ecosystem contamination.

Methods.

Study Area. Samples were collected in two protected areas in French Guiana: the Kaw-Roura National Nature Reserve (4°36′ N, 52°07′ W; 94,700 ha; ~90 km southeast of Cayenne) and the Nouragues Nature Reserve (4°05′ N, 52°41′ W; 105,000 ha) in the central-eastern region. The zones are separated by approximately 90 km straight-line distance and the Kaw River zone is a blackwater swamp whereas Nouragues consists of closed-canopy forest. A total of nine sites were surveyed, and 17 individuals were captured between 20:00 h and 01:00 h using headlamps and snares. Caimans were captured using the same field procedures as applied in previous studies (e.g. Lemaire et al., 2021a, 2022).

Microbiome and Environmental Sampling. Skin microbiomes were sampled using sterile polyester-tipped swabs. For each individual, nine swabs were passed over the entire body surface, and one swab was inserted into the cloaca and rotated. Swabs were placed immediately into sterile 2 mL tubes. Soil samples were collected from undisturbed river bank as close as possible to the capture locations by directly scooping substrate into sterile 2 mL tubes. Water was collected upstream of capture sites in sterile 50 mL Falcon tubes. Blood was collected from the occipital sinus vein using heparinized needles (27G × 16 mm for neonates; 25G × 25 mm for adults). Total length and body mass were recorded. All samples were stored in a liquid nitrogen dry shipper (-196 °C) until laboratory analyses (University of Vienna). Sampling was conducted under authorization from French authorities (Direction Générale des Territoires et de la Mer) following review by the CSRPN (Permit: R03-2022-10-20-00004).

Mercury Quantification and Blood Biochemistry. For blood mercury analysis, 1 mL whole blood was freeze-dried for 48 h and ground to a fine powder. Total Hg was quantified by direct measurement using a DMA-80 Evo III (Milestone). At least two replicates (~2.0 mg dry weight each) were analyzed per individual; duplicate reproducibility was accepted when RSD < 10%. Accuracy was verified using TORT-3 certified reference material (lobster hepatopancreas; 0.292 ± 0.022 mg g^{-1} dw), analyzed at the start and end of runs and every 10 samples (mean

recovery 101.0 ± 1.5%, n = 20). Blanks were included at the start of each run; the limit of quantification was 0.01 ng. Blood Hg is reported as μg g^{-1} dry weight.

Soil Hg was determined using the same DMA protocol, except samples were oven-dried for 72 h at 45 °C. Blood biochemistry was measured ~4 h post-sampling using a VetScan VS2 Chemistry Analyzer (Abaxis) with Avian-Reptilian and/or Preventive Care Profile Plus rotors (including alkaline phosphatase, ALP).

DNA Extraction. DNA was extracted from 177 samples (115 skin swabs, 12 cloacal swabs, 29 soils, 21 water) using the DNeasy PowerSoil HTP 96 Kit (QIAGEN), following the manufacturer's protocol except that lysis was performed in 2 mL Lysing Matrix E tubes (MPBio). DNA quantity and purity were assessed using a NanoPhotometer and Qubit 2.0 fluorometer. Extracts were cleaned using the Monarch PCR & DNA Cleanup Kit (New England Biolabs) with elution buffer pre-heated to 75 °C.

When multiple skin swabs were stored together, swabs were extracted individually due to lysis buffer absorption during bead-beating; eluates were pooled onto a single spin column at the kit elution step. Water samples were tested using centrifugation-based and direct-extraction approaches; Qubit measurements indicated DNA typically below detection (<0.5 ng μL^{-1}) and PCRs failed, so water samples were excluded from downstream sequencing.

16S rRNA Gene Sequencing. Skin swabs from 13 individuals were pooled by host, producing 13 composite skin samples, each submitted in triplicate (39 libraries), together with 28 soil samples, 11 cloacal samples, and 2 blanks. For each sample, 15 μL DNA was submitted for library preparation. The V4 region of the 16S rRNA gene was amplified using Earth Microbiome Project primers 515F (Parada) and 806R (Apprill) (515F: 5′-GTGYCAGCMGCCGCGGTAA-3′; 806R: 5′-GGACTACNVGGGTWTCTAAT-3′) and sequenced on an Illumina MiSeq (2 × 300 bp), targeting ~50,000 reads per sample.

***merA* PCR, qPCR Screening, and Cloning.** *merA* primers were synthesized (Microsynth) as 100 μM stocks and diluted to 10 μM working solutions. After gradient PCR optimization, initial amplification using Poulain et al. (2015) primers did not yield *merA* products; DNA integrity and inhibition were assessed using 16S rRNA control PCRs. *merA* detection was therefore performed using nested PCR with Wang et al. (2011) primers:

- First round (Nlf):
  Nlf-F: 5′-CCATCGGCGGCACYTGCGTYAA-3′
  Nlf-R: 5′-CGCYGCRAGCTTYAAYCYYTCRRCCATYGT-3′
- Nested round (Nsf):
  Nsf-F: 5′-ATCCGCAAGTNGCVACBGTNGG-3′
  Nsf-R: 5′-CGCYGCRAGCTTYAAYCYYTCRRCCATYGT-3′

Cycling conditions were: 98 °C for 3 min; 30 cycles of 98 °C for 10 s, 56 °C for 30 s, 72 °C for 30 s; final extension 72 °C for 5 min. Reactions (20 μL) contained 1× Phire Green Hot Start II PCR Master Mix, 200 μM each dNTP, 0.5 μM each primer, 0.4 μL Phire Hot Start II DNA polymerase, and 1 μL template DNA. Agricultural soil DNA (Montana, USA) served as a positive control. Samples failing to amplify were re-run with diluted template (2.5-10 ng DNA). Amplicons were visualized on 1% agarose gels in 0.5× TAE stained with SYBR Safe.
Five primer pairs targeting conserved *merA* regions were screened for qPCR following gradient optimization, but none produced reliable amplification in study extracts; *merA* quantification was therefore not performed.

Nested *merA* products were cloned using the pJET1.2/blunt vector system (Thermo Fisher Scientific) with a 3:1 insert-to-vector ratio, transformed into *E. coli* TOP10 by heat shock (42 °C, 45 s), recovered in SOC (37 °C, 45 min), and plated on LB-ampicillin overnight (37 °C). Inserts were screened by colony PCR with nested *merA* primers; positive products were purified (Monarch PCR & DNA Cleanup Kit) and Sanger-sequenced (Eurofins Genomics).

Bioinformatics and Statistical Analyses. Paired-end reads were processed in QIIME 2 v2024.10.1 with demultiplexing summaries (qiime demux summarize) and denoising/ASV inference using DADA2 (qiime dada2 denoise-paired) with truncation lengths of 200 bp (forward) and 180 bp (reverse). Technical replicates were merged by summing counts (qiime feature-table group). Taxonomy was assigned using a Naïve Bayes classifier trained on SILVA 138 trimmed to the same read lengths (classify-sklearn). Putative non-target features (mitochondria, chloroplasts, Eukaryota, and unassigned) were removed prior to downstream analyses. Statistical analyses were conducted in R, including Hellinger transformation of relative abundances (vegan::decostand), Bray-Curtis dissimilarities (vegan::vegdist), and multivariate and differential-abundance workflows. Additional bioinformatic and analysis details are available upon reasonable request.

Mercury Binning: Categorizing Samples based on Mercury Levels. To examine differences in microbiome composition across mercury exposure levels, samples were categorized into "High" and "Low" mercury groups based on the median mercury concentration within each dataset. For soil and skin microbiome datasets, binning was performed using soil mercury concentration (Soil_Hg), while for the cloacal microbiome dataset, binning was based on whole blood mercury concentration. For each dataset, the median value was calculated using median(na.rm = TRUE) in R, and samples with concentrations greater than the median were assigned to the "High" group, while those at or below the median were assigned to the "Low" group. Samples lacking mercury measurements were assigned an "NA" category and excluded from subsequent bin-based comparisons.

Results.

Sample Description and Demographics. Across 15 captures, we measured total length (TL) and body mass for 12 *P. trigonatus* and 3 *M. niger* individuals.

In *P. trigonatus*, TL ranged from 26.4 to 140.0 cm (M = 111.0 SD = 30.7; n = 12) and body mass from 410.0 to 15200.0 g (7103.2 ± 4784.0; n = 11). The body mass from one individual wasn't recorded.

In *M. niger*, TL ranged from 109.0 to 146.0 cm (129.7 ± 18.9; n = 3) and body mass from 2600.0 to 8150.0 g (5700.0 ± 2831.5; n = 3). Whole-blood Hg averaged 0.68 ± 0.42 μg g^{-1} across all sampled individuals (n = 15), 0.53 ± 0.22 μg g^{-1} in *P. trigonatus* (n = 12), and 1.25 ± 0.60 μg g^{-1} in *M. niger* (n = 3).

Across all soil samples, the mean Hg concentration was 0.144 μg g^{-1} (n = 9). By zone, Nouragues had a median of 0.163 μg g^{-1} (IQR = 0.051, n = 7), while Petit Saut and Kaw were represented by single samples (0.140 and 0.126 μg g^{-1}, respectively), precluding SD/IQR estimation. A Kruskal-Wallis test indicated no difference among zones ($\chi^2 = 1.15$, df = 2, p = 0.564).

Species	Zone	Place	Place	Number of individuals sampled per species
M. niger	Kaw	Mare Agami	3	3
P. trigonatus	Nouragues	C. Cascades	3	12
		C. Montagne Russe	1	
		C. Nouragues	3	
		Layon museum	2	
	Petit Saut	Dame du Lac	1	
		Marie Hilaire	1	
		Sud Dame du lac	1	
Total number of individuals sampled				15

Sequencing results and quality. Sequencing produced 80 libraries with balanced paired-end yields (forward = reverse = 2,715,083 reads). Per-library depth ranged from 8 to 65,267 reads (median = 35,829; mean = 34,368). After DADA2 denoising/merging and ASV inference, 1,154,745 sequences were assigned to 12,214 ASVs using the SILVA-138 classifier. Taxonomic filtering removed non-target/ambiguous annotations: Unassigned (432,451 reads; 4,659 ASVs), Eukaryota (85,366; 604), mitochondria (34,115; 965), and chloroplasts (29,011; 148). The retained bacterial/archaeal fraction comprised 573,802 reads (49.7% of post-DADA2 reads) across 5,838 ASVs (47.8% of ASVs).

Phylum-level community composition across environments, hosts, and location.
Across all samples, 50 phylum-level taxa were detected; 41 named bacterial/archaeal phyla and 9 candidate/unclassified groups. By environment, cloaca samples were enriched in Pseudomonadota (27%), Bacteroidota (23%), Bacillota (17%), and Actinomycetota (12%); skin harbored Pseudomonadota (30%), Cyanobacteriota (19%), and Actinomycetota (11.9%); soils were characterized by Pseudomonadota (25%), Acidobacteriota (14%), and Actinomycetota (12%). By host species, *M. niger* showed a Pseudomonadota-dominated profile (41%) with Cyanobacteriota (19%) and Actinomycetota (12%), whereas *P. trigonatus* had lower Pseudomonadota (24%) and higher Acidobacteriota (10%) and Bacteroidota (10%). Pseudomonadota dominated in all the environments (cloaca, skin and soil, 24.8-26.6%) as well as a large proportion of Actinomycetota (11.4-13%). Of the Pseudomonadota, Gammaproteobacteria represented one of the most abundant classes across all environments (Cloaca: 23.3%, Skin 9.4%, Soil: 9.02%), followed by Alphaproteobacteria, particularly in soil samples (Cloaca: 3.4%, Skin 9.2%, Soil: 14.92%). Bacteroidia (Phylum Bacteroidota) represented a substantial component of host-associated samples (Cloaca: 22.6%, Skin: 14.4%) while remaining minimal in environmental soils (3.5%). The skin and cloacal microbiomes of caimans exhibit a distinctive host-associated signature characterized by a core community dominated by Bacteroidia and Bacillota, with Fusobacteria serving as a defining crocodilian

hallmark. Fusobacteria detection in cloacal and skin samples was 0.9% and 0.6% respectively. Bacillota also represented a consistent fraction of the communities (Cloaca: 16.0%, Skin: 5.3%, Soil: 8.1). In addition to these major phyla, Synergistota were recovered in low abundance overall (Cloaca: 1.45%, Skin: 0.2%, Soil: not detected) but was detected in over 50% of the cloacal samples. The skin microbiome included Pseudomonadota (29.5%), Cyanobacteriota (19.1%), and Actinomycetota (11.9%), but with an absence of the large Bacteroidota and Bacillota fractions found in the cloaca. Two specialized phyla, Deinococcota and Armatimonadota, were detected in over 50% of all skin samples.

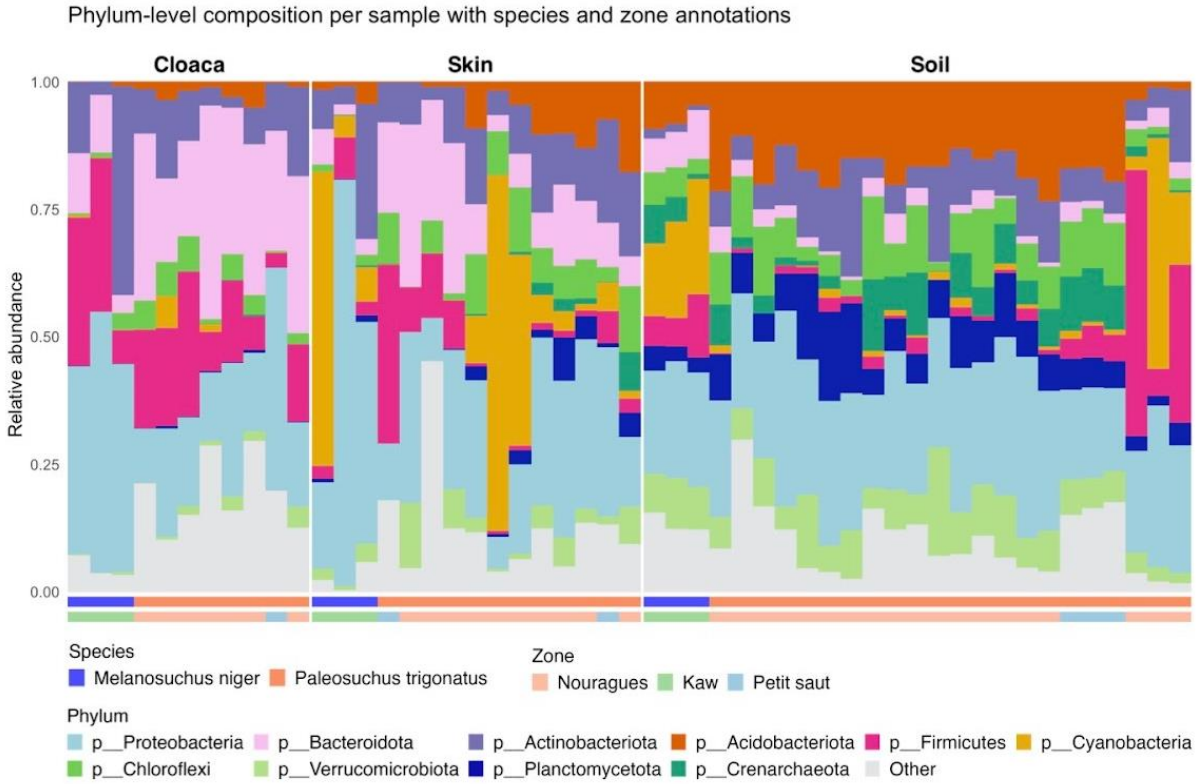


Figure 1: Phylum-level community composition per sample across three compartments (cloaca, skin, soil). Stacked bars show relative abundances for individual samples; colors denote phyla, with "Other" aggregating low-abundance taxa. Samples are annotated by host species (M. niger, P. trigonatus) and zone (Nouragues, Kaw, Petit Saut). Profiles differ by compartment, with soils enriched for Acidobacteriota/Actinomycetota and host sites dominated by Proteobacteria and Bacteroidota. Plot labels show legacy phylum names, in the text we use the updated NCBI nomenclature: Proteobacteria → Pseudomonadota, Actinobacteriota → Actinomycetota, Firmicutes → Bacillota, Cyanobacteria → Cyanobacteriota.

Alpha diversity remains stable between low and high mercury samples across cloaca, skin and soil.

To assess how the microbial community properties changed between high and low mercury we compared Observed richness, Shannon diversity and Evenness across the cloaca, skin and soil. Wilcoxon tests indicated no statistically significant differences in alpha diversity metrics between low and high mercury groups within any of the environments (Cloaca: observed richness: $p_{adj} = 0.222$; Shannon: $p_{adj} = 0.0952$; evenness: $p_{adj} = 0.0686$; Skin: observed richness: $p_{adj} = 0.222$; Shannon: $p = 0.429$; evenness: $p_{adj} = 0.73$; Soil: observed richness: $p_{adj} = 0.222$; Shannon: $p_{adj} = 0.769$; evenness: $p_{adj} = 0.0686$)(Figure 2). Although not significant, the following trends were observed. Low mercury cloaca samples were more diverse than high in the cloaca and soil (Cloaca: 142 ± 26.0 vs 118 ± 58.6 ASVs; Soil:198 ± 97.4 vs 131 ± 46.3

ASVs). Skin samples showed the opposite trend and increased richness under high mercury (362 ± 111.0 vs 257 ± 123.0 ASVs). Shannon diversity decreased with mercury in the cloaca (Shannon 3.93 ± 0.262 vs 3.24 ± 0.666), remained stable in soil and skin (Soil: Shannon diversity: 4.49 ± 0.857 vs 4.52 ± 0.351; Skin: Evenness 0.835 ± 0.0419 vs 0.799 ± 0.107).

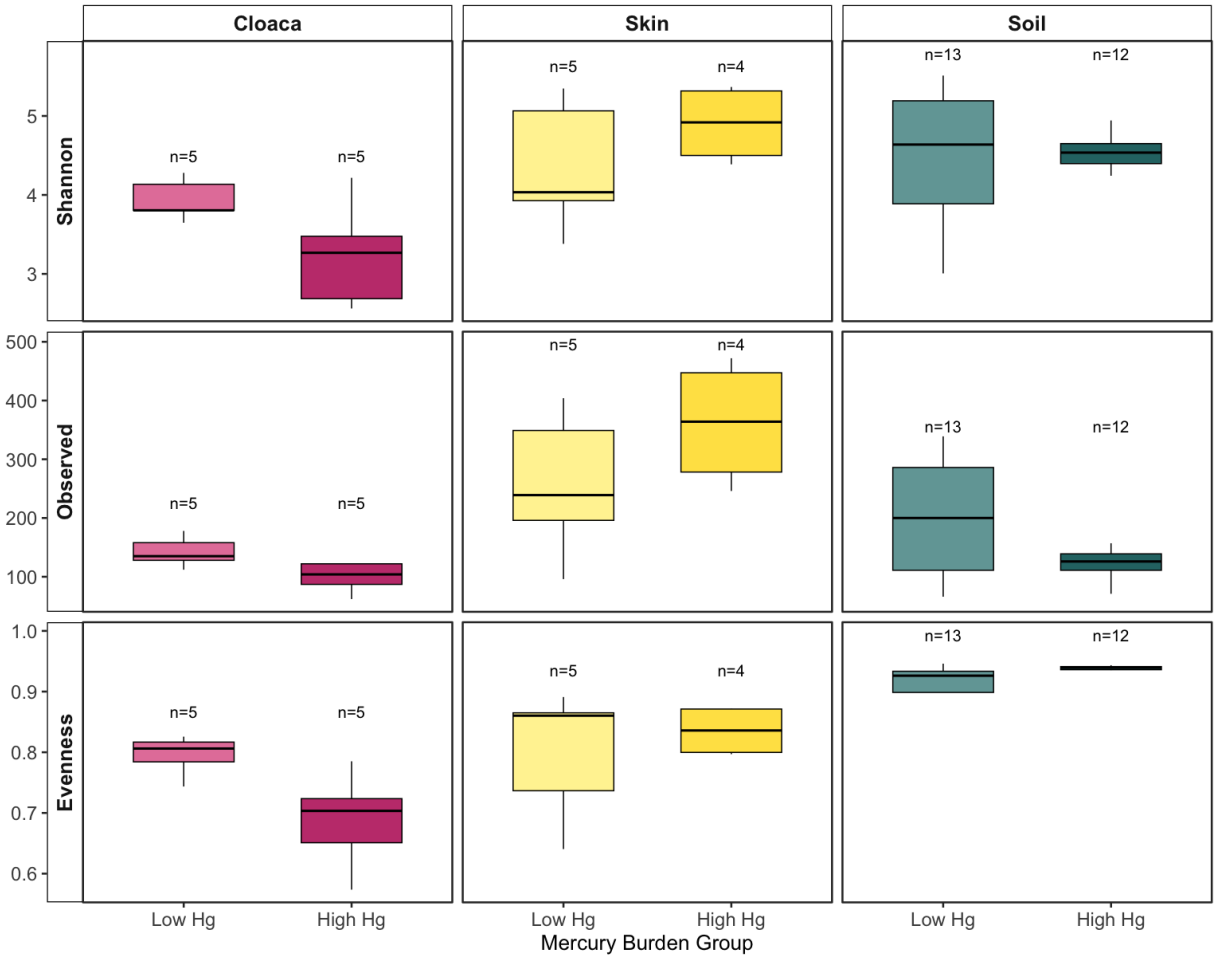


Figure 2: Alpha diversity of cloacal, skin, and soil microbiomes across low- and high-mercury (Hg) burden groups. Boxplots show Shannon diversity, observed amplicon sequence variant (ASV) richness, and Pielou's evenness for each compartment. Boxes indicate medians and interquartile ranges; whiskers extend to 1.5 × IQR. Sample sizes are shown above boxes.

Environmental (soil) microbiomes are organized by mercury and geographic location; host-associated (cloaca, skin) microbiomes are comparatively robust.

Mercury effects on microbial community composition were evaluated using PERMANOVA, PERMDISP, and constrained ordination analyses. In host-associated microbiomes, mercury was not significantly associated with community composition in either skin (PERMANOVA $R^2 = 0.104$, $p = 0.056$) or cloaca ($R^2 = 0.129$, $p = 0.246$), and group dispersions were homogeneous in both compartments (PERMDISP: skin $p = 0.543$; cloaca $p = 0.129$). In contrast, soil communities differed between mercury exposure groups (PERMANOVA $R^2 = 0.096$, $p = 0.001$), although dispersions were also heterogeneous (PERMDISP $p = 0.040$), indicating that differences reflected both centroid separation and variability. Redundancy analysis of soil microbiomes ($n = 25$) showed that spatial context was the dominant structuring factor, with Zone explaining 17.86% of partial inertia (21.10% of total inertia; $F = 3.087$,

p = 0.001), while mercury burden contributed an additional independent fraction (6.04% partial inertia; 7.14% of total inertia; F = 2.089, p = 0.003). Ordination plots showed primary separation by Zone, with a secondary gradient aligned with mercury.

When restricting the analysis to soils associated with *P. trigonatus*, the global RDA was significant (constrained inertia = 0.325; adjusted R^2 = 0.205; F = 2.08, p = 0.001), with significant partial effects of Place (25.60%; F = 2.05, p = 0.001) and Hg_burden (7.00%; F = 2.25, p = 0.001). Variation partitioning analysis corroborated these results, identifying Place as the dominant factor (adjusted R^2 = 0.214, p = 0.001) and mercury as a smaller but significant component (adjusted R^2 = 0.037, p = 0.001). In host-associated communities, joint analysis of skin and cloaca yielded a significant constrained ordination (R^2 = 0.25, F = 1.17, p = 0.036), but marginal tests did not detect significant unique effects of mercury, body condition, or geography (all p > 0.23), and separate analyses of skin and cloaca likewise showed no significant unique predictors (all marginal p ≥ 0.275). Collectively, these results indicate that soil microbiomes are primarily structured by geography, with mercury contributing an additional independent signal, whereas host-associated microbiomes are comparatively robust to mercury exposure within the sampled range.

Host-associated co-occurrence network topology remained stable under high Hg, whereas soil networks contracted.

Co-occurrence networks at the genus level were built using Spearman's correlations between taxa abundances, keeping all strong positive and negative relationships ($|\rho| \geq 0.65$, $p < 0.05$) to capture both cooperative and competitive interactions. At the genus level, network topology of host-associated microbiomes (cloaca and skin) remained consistent across mercury bins, whereas the soil microbiome network exhibited substantial contraction under high Hg (Figure 3). For the cloacal microbiome, the low-Hg network comprised 34 genera and 24 edges (global clustering coefficient = 1.0; modularity = 0.885; 15 modules). Under high Hg, the network expanded to 42 nodes and 77 edges with comparable clustering (1.0) and slightly reduced modularity (0.630; 13 modules). Differences in density, clustering, modularity, and positive-edge ratio were not significant (all p ≥ 0.133). In the skin microbiome, the low-Hg network included 98 genera and 282 edges (clustering = 0.950; modularity = 0.790). The high-Hg network contained 124 genera and 412 edges (clustering = 1.0; modularity = 0.847). No significant differences were detected for any global property (all p ≥ 0.121). The soil microbiome displayed distinct topological changes between Hg categories. Under low Hg, the network consisted of 118 genera and 383 edges (clustering = 0.629; modularity = 0.537). Under high Hg, it contracted to 44 nodes and 38 edges, with higher clustering (0.857) and modularity (0.878). Node and edge numbers were significantly lower in the high-Hg network (p = 0.002 and p = 0.001, respectively). Overall, these data indicate that mercury exposure did not affect the global network organization of host-associated microbiomes, whereas soil networks exhibited reduced complexity and connectivity under high Hg conditions.

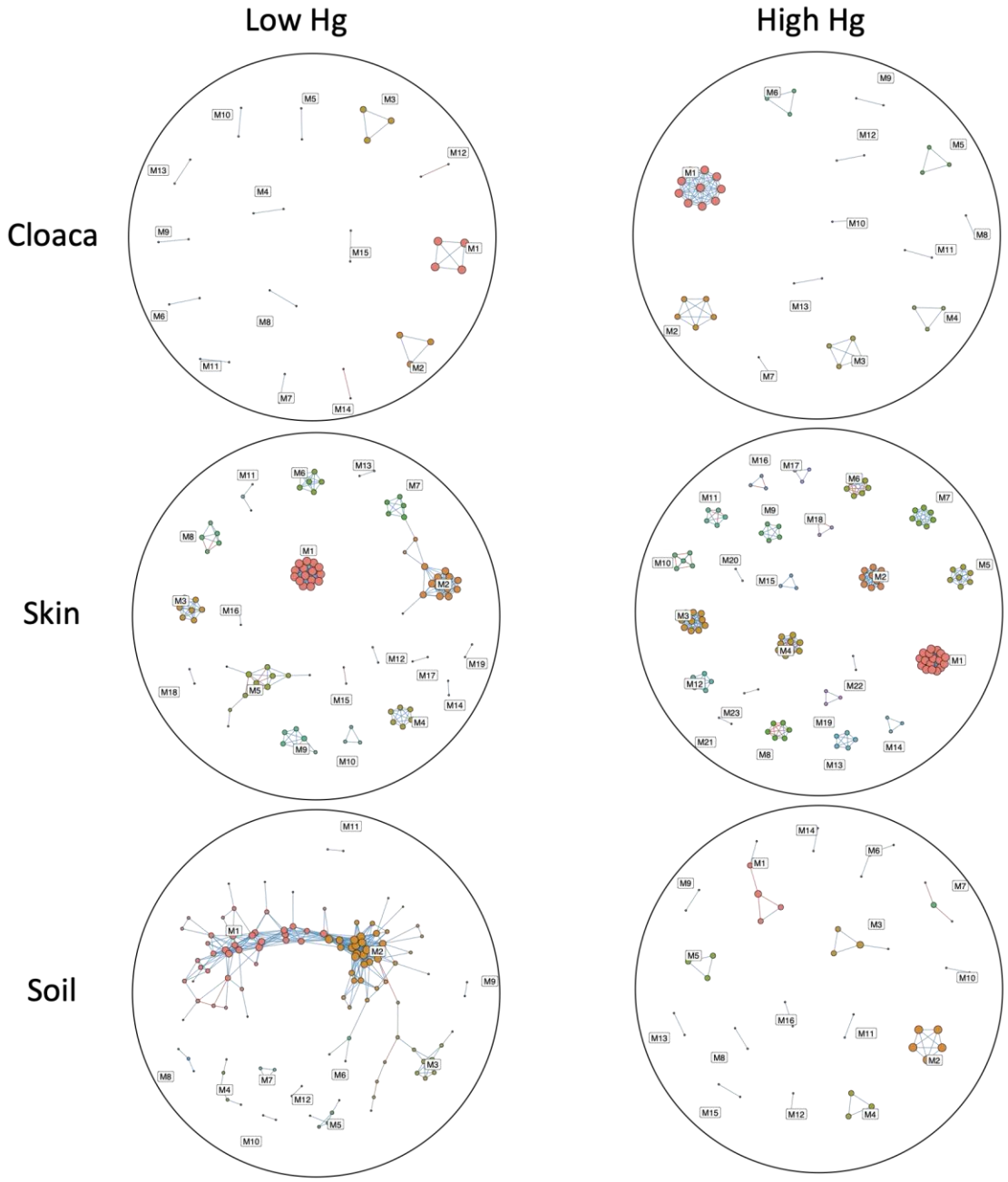


Figure 3: Genus-level co-occurrence network diagrams for cloacal (top panels), skin (middle panels), and soil (bottom panels) microbiomes under low (left panels) and high (right panels) mercury (Hg) exposure. In each panel, nodes represent microbial genera and edges represent significant positive or negative correlations (Spearman's $\rho > |0.65|$, $p < 0.01$) between taxa abundances; colors indicate module membership. Panels for cloaca and skin show consistent network structure between Hg categories, while panels for soil illustrate marked network contraction and reduced connectivity under high Hg conditions.

MerA detection showed no relationship with mercury levels at either the site or the individual scale.

Qualitative PCR targeting *merA* showed a lower detection rate in *M. niger* cloacal samples (1/3 positive) compared with P. trigonatus (5/9 positive), despite *M. niger* carrying a higher mercury burden in whole blood (Mdn = 0.66 ug g-1) compared to *P. trigonatus* (Mdn = 0.14 ug g-1) (Wilcoxon W = 42, p = 0.013)(Table 1). While the small sample size prevents robust statistical

conclusions, this suggests that *P. trigonatus* may harbor greater potential for microbial mercury resistance in the cloaca.

The soil sample associated with *M. niger* (three replicates) all tested negative for *merA* presence whereas *merA* was detected in all of soil samples associated with *P. trigonatus*, in at least 2/3 and 3/4 replicates. Across sites, soil-Hg was not associated with the proportion of *merA*-positive samples (Pearson r = 0.16, p = 0.68; Spearman ρ = 0.36, p = 0.34; n = 9). *M. niger* were captured in the Kaw zone whereas *P. trigonatus* were captured in Nouragues.

For the cloaca samples only 1/3 *M. niger* individuals tested positive for *merA* presence whereas *merA* was detected in cloaca samples of 5/9 *P. trigonatus* individuals. Similar to soil-Hg, whole-blood Hg did not predict *merA* positivity in *M. niger* cloaca (Pearson r = -0.69, p = 0.51; Spearman ρ = -0.87, p = 0.33) or skin (Pearson r = 0.28, p = 0.82; Spearman ρ = 0, p = 1), nor in *P. trigonatus* cloaca (Pearson r = 0.29, p = 0.48; Spearman ρ = 0.28, p = 0.50) or skin (Pearson r = 0.30, p = 0.43; Spearman ρ = 0.21, p = 0.59). Collectively, there was no detectable linear or monotonic association between mercury exposure and *merA* detection within the sampled range. While the small sample size prevents robust statistical conclusions, this suggests that *P. trigonatus* may harbor greater potential for microbial mercury resistance in the cloaca. One possible explanation lies in the distinct ecologies of the two species: *P. trigonatus* is semi-terrestrial, inhabiting forest streams and terrestrial refuges, while *M. niger* is primarily aquatic, restricted to swamps and blackwater rivers. These habitat differences may influence the pool of environmental bacteria that seed the cloaca. Indeed, Smith et al. (2021) showed that microbial communities in reptiles vary significantly with habitat type, with body-site assemblages diverging between marine, semi-arboreal, and arboreal species. It is therefore plausible that the semi-terrestrial lifestyle of *P. trigonatus* exposes it to a broader or more metal-tolerant set of environmental taxa, which are then incorporated into its cloacal microbiome, compared to the more aquatic *M. niger*.

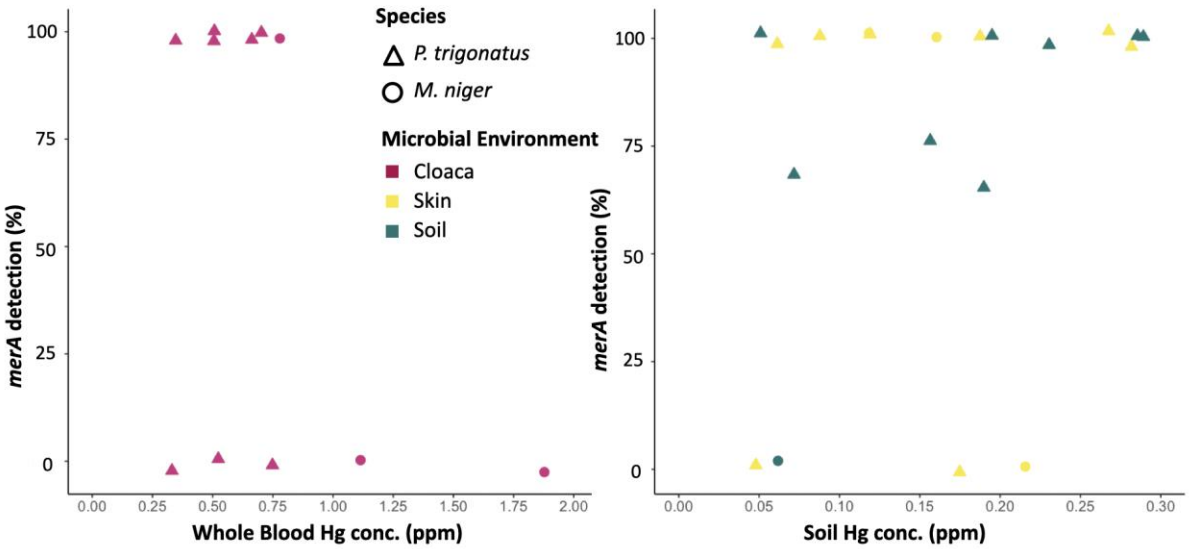


Figure 4: Detection frequency of the mercury resistance gene merA in host-associated and environmental microbiomes in relation to mercury exposure. Left panel shows merA detection (%) as a function of whole-blood mercury concentration (ppm) for cloacal samples, with symbols indicating host species (P. trigonatus, triangles; M. niger, circles). Right panel shows merA detection (%) in relation to soil mercury concentration (ppm) for soil, skin, and cloacal-associated environments. Point colors indicate microbial environment (cloaca, skin, soil). merA detection was binary at the sample level and is displayed as presence (100%) or absence (0%). No clear relationship was observed between mercury concentration and merA detection across hosts or compartments within the sampled mercury range.

Discussion and Conclusion.

This study provides an integrated analysis of cloacal, skin, and soil microbiomes associated with the Neotropical caimans *M. niger* and *P. trigonatus* across a mercury contamination gradient in French Guiana. Microbial community structure was primarily determined by environmental compartment and spatial context, with additional but compartment-specific effects of host species identity. Mercury exposure exerted distinct effects across compartments, strongly influencing soil communities while having comparatively weak effects on host-associated microbiomes.

Across all compartments, alpha diversity metrics did not differ significantly between high- and low-mercury groups. Nevertheless, consistent trends emerged. Cloacal microbiomes tended toward reduced diversity at higher mercury exposure, skin microbiomes showed increased richness, and soil communities exhibited mixed responses depending on the diversity metric considered. These contrasting responses highlight the importance of ecological context and exposure routes in shaping microbial stress responses. While metal contamination often reduces alpha diversity, increased diversity under stress can reflect destabilization, where opportunistic and transient taxa inflate richness without enhancing functional stability. The increase in skin diversity under higher mercury exposure may therefore indicate weakened host control at this exposed interface rather than improved resilience.

In wild *Crocodylus porosus* from northern Australia, Scheelings et al. (2025) reported cloacal communities dominated by Pseudomonadota (54.5%), whereas captive individuals showed a pronounced shift toward Bacteroidota dominance (77.8%). In contrast, cloacal microbiomes of the wild caimans sampled in this study from French Guiana displayed a more even phylum-level structure, with Pseudomonadota (27%), Bacteroidota (23%), and Bacillota (17%) present at comparable relative abundances, together with a substantial contribution of Actinomycetota (12%). Although Pseudomonadota was the most abundant phylum in both wild *C. porosus* and the wild caimans sampled in this study, its dominance was markedly reduced in the latter, and no single phylum reached the levels observed under captive conditions. In *Alligator mississippiensis*, cloacal and intestinal microbiomes are often enriched in Fusobacteriota and Bacillota, with lower relative contributions of Pseudomonadota (Keenan et al., 2013; Keenan and Elsey, 2015; Kieran et al., 2020). In the wild caimans sampled in this study, Fusobacteriota were consistently present but did not dominate. Together, these contrasts suggest that crocodilian cloacal microbiomes could share a common set of core phyla, but differ in their relative balance, likely reflecting species-specific ecology, environmental exposure, and captivity effects.

Skin and soil microbiomes were dominated by external filters. Skin communities were shaped mainly by geographic location, consistent with the skin acting as a transient interface repeatedly inoculated by local water and sediments. Soil microbiomes clustered by site and responded clearly to mercury exposure, despite the relatively narrow concentration range sampled. These findings support the view that free-living microbial communities are more directly sensitive to environmental contaminants, whereas host-associated niches are partially buffered by host physiology.

Co-occurrence network analyses highlighted differences between environmental and host-associated microbiomes. Soil microbial networks differed between lower- and higher-mercury groups, with reduced connectivity and redundancy in soils associated with higher mercury concentrations. These patterns should be interpreted cautiously, as mercury co-varies with

other unmeasured environmental factors, including vegetation, soil type, organic matter content, and hydrology, which likely also contribute to differences in soil microbial communities. In contrast, skin and cloacal networks showed relatively stable topological properties across mercury categories, suggesting that host-associated microbial interactions are less sensitive to environmental variation than free-living soil communities, even when taxonomic turnover occurs.

The mercury resistance gene *merA* was detected irregularly across soils, skin, and cloaca, but showed no clear relationship with mercury concentrations. This patchy distribution suggests microhabitat-level selection driven by fine-scale heterogeneity in mercury bioavailability rather than uniform adaptation. Anoxic conditions, chemical precipitation, or alternative mercury reduction pathways may reduce selective pressure for *merA* maintenance in some microenvironments. The lack of correlation also highlights limitations of single-gene screening, as *merA* presence alone does not reliably indicate functional mercury resistance.

A limitation of the study is that total mercury was measured in the soil however the chemical form of mercury and therefore the bioavailability is influenced by environmental factors such as dissolved organic matter, pH, and salinity (Frey and Rieder, 2013; Frossard et al., 2017; Eagles-Smith et al., 2018). Therefore, abiotic conditions can modulate the selective pressure exerted by mercury in soil and the limited microbiome responses we observed could reflect this limitation and the relatively narrow mercury ranges in our dataset. So although for the purpose of this study we separated the samples into low and high groups it is important to remember that these do not represent uncontaminated vs highly contaminated environments, rather they contrast the lower and upper samples of a small range of mercury contaminated samples. Whole-blood Hg in caimans ranged from 0.20 to 1.91 ppm (mean 0.71 ppm, n = 18). Values were highest in *M. niger* (max = 1.91 ppm) but overlapped with *P. trigonatus*; between-species tests were not significant for blood Hg ($W = 19$, $p = 1$) or site soils ($W = 2$, $p = 0.6$), noting the small M. niger sample size (n = 3). Soils averaged 0.14 µg g^{-1} (0.049–0.207 µg g^{-1}, n = 9), highest at Crique Nouragues (median 0.207) and lowest at Layon Museum (0.049). These concentrations fall within the low to moderate range reported regionally, lower than typical values from mining-affected Guyana soils (0.215 ± 0.187 µg g^{-1} overall; 0.226 ± 0.171 in mining areas; 0.187 ± 0.077 in conservation areas; Howard et al., 2011) and within French Guiana expectations of about 0.1-0.3 µg g^{-1} depending on soil type (Richard et al., 2000). Consequently, our “high” and “low” bins represent relative differences within a narrow gradient rather than clean versus heavily contaminated sites.

Overall, these results demonstrate that geography and compartment-specific ecology dominate microbiome assembly in caimans, while mercury primarily restructures free-living soil communities. Host-associated microbiomes appear buffered against mercury-induced disruption, and functional inference based solely on *merA* detection is insufficient. Future work should integrate multi-gene screening, functional assays, and bioavailable mercury measurements to better resolve microbiome-mediated mercury detoxification in natural systems. In addition, incorporating local abiotic factors and ecological context would be advantageous, including soil pH, organic matter content, soil texture, hydrology, and temperature.

Acknowledgements.
This work was supported by funding from the IUCN SSC Crocodile Specialist Group Student Research Assistance Scheme (SRAS) as well as by the University of Vienna through the Postdoctoral Research Seed Grant and the Short-term Grants Abroad (KWA). I thank Jérémy Lemaire, Rosanna Mangione, Zhen-Hao Luo, Melina Kerou, Marina Monserrat-Díez, Filipa Sousa, Christa Schleper for supervision, project conception and for fostering an interdisciplinary research environment at the University of Vienna.

Literature Cited.

AMAP. (2021). *AMAP assessment 2021: Mercury in the Arctic*. Arctic Monitoring and Assessment Programme. https://www.amap.no/

Anderson, J. R. (1999). *Characterisation of the oral and cloacal flora of wild and farmed crocodiles (Crocodylus porosus and C. johnstoni) in northern Australia* (Honours thesis). James Cook University of North Queensland.

Anderson, M. J. (2001). A new method for non-parametric multivariate analysis of variance. *Austral Ecology, 26*(1), 32-46. https://doi.org/10.1111/j.1442-9993.2001.01070.pp.x

Anderson, M. J. (2006). Distance-based tests for homogeneity of multivariate dispersions. *Biometrics, 62*(1), 245-253. https://doi.org/10.1111/j.1541-0420.2005.00440.x

Apprill, A., McNally, S., Parsons, R., & Weber, L. (2015). Minor revision to V4 region SSU rRNA 806R gene primer greatly increases detection of SAR11 bacterioplankton. *Frontiers in Microbiology, 6*, 1480. https://doi.org/10.3389/fmicb.2015.01480

Barkay, T., & Gu, B. (2021). Demethylation—the other side of the mercury methylation coin: A critical review. *ACS Environmental Au, 2*(2), 77-97. https://doi.org/10.1021/acsenvironau.1c00011

Barkay, T., Miller, S. M., & Summers, A. O. (2003). Bacterial mercury resistance from atoms to ecosystems. *FEMS Microbiology Reviews, 27*(2-3), 355-384. https://doi.org/10.1016/S0168-6445(03)00046-9

Benjamini, Y., & Hochberg, Y. (1995). Controlling the false discovery rate: A practical and powerful approach to multiple testing. *Journal of the Royal Statistical Society: Series B (Methodological), 57*(1), 289-300.

Bolyen, E., Rideout, J. R., Dillon, M. R., Bokulich, N. A., Abnet, C. C., Al-Ghalith, G. A., Alexander, H., Alm, E. J., et al. (2019). Reproducible, interactive, scalable and extensible microbiome data science using QIIME 2. *Nature Biotechnology, 37*(8), 852-857. https://doi.org/10.1038/s41587-019-0209-9

Borcard, D., Legendre, P., & Drapeau, P. (1992). Partialling out the spatial component of ecological variation. *Ecology, 73*(3), 1045-1055. https://doi.org/10.2307/1940179

Bray, J. R., & Curtis, J. T. (1957). An ordination of the upland forest communities of southern Wisconsin. *Ecological Monographs, 27*(4), 325-349. https://doi.org/10.2307/1942268

Callahan, B. J., McMurdie, P. J., Rosen, M. J., Han, A. W., Johnson, A. J. A., & Holmes, S. P. (2016). DADA2: High-resolution sample inference from Illumina amplicon data. *Nature Methods, 13*(7), 581-583. https://doi.org/10.1038/nmeth.3869

Caut, S., François, V., Bacques, M., Guiral, D., Lemaire, J., Lepoint, G., Marquis, O., & Sturaro, N. (2019). The dark side of the black caiman: Shedding light on species dietary ecology and movement in Agami Pond, French Guiana. *PLOS ONE, 14*(5), e0217239. https://doi.org/10.1371/journal.pone.0217239

Charruau, P., Pérez-Flores, J., Pérez-Juárez, J., Cedeño-Vázquez, J., & Rosas-Carmona, R. (2012). Oral and cloacal microflora of wild crocodiles *Crocodylus acutus* and *C. moreletii* in the Mexican Caribbean. *Diseases of Aquatic Organisms, 98*(1), 27-39. https://doi.org/10.3354/dao02418

Chen, C. Y., Driscoll, C. T., Eagles-Smith, C. A., Eckley, C. S., Gay, D. A., Hsu-Kim, H., Keane, S. E., Kirk, J. L., Mason, R. P., Obrist, D., Selin, H., Selin, N. E., & Thompson, M. R. (2018). A critical time for mercury science to inform global policy. *Environmental Science & Technology, 52*(17), 9556-9561. https://doi.org/10.1021/acs.est.8b02286

Christakis, C. A., Barkay, T., & Boyd, E. S. (2021). Expanded diversity and phylogeny of *mer* genes broadens mercury resistance paradigms and reveals an origin for MerA among thermophilic archaea. *Frontiers in Microbiology, 12*, 682605. https://doi.org/10.3389/fmicb.2021.682605

Coyte, K. Z., Schluter, J., & Foster, K. R. (2015). The ecology of the microbiome: Networks, competition, and stability. *Science, 350*(6261), 663-666. https://doi.org/10.1126/science.aad2602

Driscoll, C. T., Mason, R. P., Chan, H. M., Jacob, D. J., & Pirrone, N. (2013). Mercury as a global pollutant: Sources, pathways, and effects. *Environmental Science & Technology, 47*(10), 4967-4983. https://doi.org/10.1021/es305071v

Eagles-Smith, C. A., Silbergeld, E. K., Basu, N., Bustamante, P., Diaz-Barriga, F., Hopkins, W. A., Kidd, K. A., & Nyland, J. F. (2018). Modulators of mercury risk to wildlife and humans in the context of rapid global change. *Ambio, 47*(2), 170-197. https://doi.org/10.1007/s13280-017-1011-x

Escallón, C., Belden, L. K., & Moore, I. T. (2019). The cloacal microbiome changes with the breeding season in a wild bird. *Integrative Organismal Biology, 1*(1), oby009. https://doi.org/10.1093/iob/oby009

Esdaile, L. J., & Chalker, J. M. (2018). The mercury problem in artisanal and small-scale gold mining. *Chemistry - A European Journal, 24*(27), 6905-6916. https://doi.org/10.1002/chem.201704840

Flandry, F., Lisecki, E. J., Domingue, G. J., Nichols, R. L., Greer, D. L., & Haddad, R. J. (1989). Initial antibiotic therapy for alligator bites: Characterization of the oral flora of *Alligator mississippiensis*. *Southern Medical Journal, 82*(2), 262-266.

Frey, B., & Rieder, S. R. (2013). Response of forest soil bacterial communities to mercury chloride application. *Soil Biology and Biochemistry, 65*, 329-337. https://doi.org/10.1016/j.soilbio.2013.06.001

Frossard, A., Donhauser, J., Mestrot, A., Gygax, S., Bååth, E., & Frey, B. (2018). Long- and short-term effects of mercury pollution on the soil microbiome. *Soil Biology and Biochemistry, 120*, 191-199. https://doi.org/10.1016/j.soilbio.2018.01.028

Gu, B., Bian, Y., Miller, C. L., Dong, W., Jiang, X., & Liang, L. (2011). Mercury reduction and complexation by natural organic matter in anoxic environments. *Proceedings of the*

National Academy of Sciences of the United States of America, 108(4), 1479-1483. https://doi.org/10.1073/pnas.1008747108

Howard, J., Trotz, M. A., Thomas, K., Omisca, E., Chiu, H. T., Halfhide, T., Akiwumi, F., Michael, R., & Stuart, A. L. (2011). Total mercury loadings in sediment from gold mining and conservation areas in Guyana. *Environmental Monitoring and Assessment, 179*, 555-573. https://doi.org/10.1007/s10661-010-1762-3

Keenan, S. W., Engel, A. S., & Elsey, R. M. (2013). The alligator gut microbiome and implications for archosaur symbioses. *Scientific Reports, 3*, 2877. https://doi.org/10.1038/srep02877

Keenan, S. W., & Elsey, R. M. (2015). The good, the bad, and the unknown: Microbial symbioses of the American alligator. *Integrative and Comparative Biology, 55*(6), 972-985. https://doi.org/10.1093/icb/icv006

Kieran, T. J., Goodman, S. J., Finger, J. W., Thomas, J. C., Hamilton, M. T., Tuberville, T. D., & Glenn, T. C. (2020). Microbiota of four tissue types in American alligators (*Alligator mississippiensis*) following extended dietary selenomethionine exposure. *Bulletin of Environmental Contamination and Toxicology, 105*(3), 381-386. https://doi.org/10.1007/s00128-020-02961-3

Legendre, P., & Gallagher, E. D. (2001). Ecologically meaningful transformations for ordination of species data. *Oecologia, 129*(2), 271-280. https://doi.org/10.1007/s004420100716

Lemaire, J. (2023). Using crocodylians for monitoring mercury in the tropics. *Ecotoxicology, 32*(8), 977-993. https://doi.org/10.1007/s10646-023-02703-1

Lemaire, J., Bustamante, P., Marquis, O., Caut, S., & Brischoux, F. (2021a). Influence of sex, size, and trophic level on blood mercury concentrations in black caiman (Melanosuchus niger) from French Guiana. Chemosphere, 262, 127819. https://doi.org/10.1016/j.chemosphere.2020.127819

Lemaire, J., Bustamante, P., Marquis, O., Caut, S., & Brischoux, F. (2021b). Maternal transfer of mercury in smooth-fronted caiman (Paleosuchus trigonatus). Environmental Research, 194, 110494. https://doi.org/10.1016/j.envres.2020.110494

Lemaire, J., Brischoux, F., Marquis, O., Mangione, R., Caut, S., Brault-Favrou, M., Churlaud, C., & Bustamante, P. (2022). Relationships between stable isotopes and trace elements in a crocodilian community. *Science of the Total Environment, 837*, 155846. https://doi.org/10.1016/j.scitotenv.2022.155846

Lemaire, J., Mangione, R., Caut, S., & Bustamante, P. (2024). Mercury biomagnification in the food web of Agami Pond, Kaw-Roura Nature Reserve, French Guiana. *Heliyon, 10*(7), e28859. https://doi.org/10.1016/j.heliyon.2024.e28859

Mathema, V. B., Thakuri, B. C., & Sillanpää, M. (2011). Bacterial *mer* operon-mediated detoxification of mercurial compounds: A short review. *Archives of Microbiology, 193*(12), 837-844. https://doi.org/10.1007/s00203-011-0751-4

Müller, A. K., Westergaard, K., Christensen, S., & Sørensen, S. J. (2001a). The effect of long-term mercury pollution on the soil microbial community. *FEMS Microbiology Ecology, 36*(1), 11-19. https://doi.org/10.1111/j.1574-6941.2001.tb00821.x

Müller, A. K., Rasmussen, L. D., & Sørensen, S. J. (2001b). Adaptation of the bacterial community to mercury contamination. *FEMS Microbiology Letters, 204*(1), 49-53.

Nascimento, A. M. A., & Chartone-Souza, E. (2003). Operon *mer*: Bacterial resistance to mercury and potential for bioremediation of contaminated environments. *Genetics and Molecular Research, 2*(1), 92-101.

Núñez-Otaño, N. B., Ignacio Piña, C., Gonçalves Portelinha, T. C., & Arambarri, A. M. (2013). Cloacal mycobiota in wild females of *Caiman latirostris* (Crocodylia: Alligatoridae). *Revista Mexicana de Biodiversidad, 84*(2), 722-726. https://doi.org/10.7550/rmb.32425

Oksanen, J., Simpson, G. L., Blanchet, F. G., Kindt, R., Legendre, P., Minchin, P. R., O'Hara, R. B., Simpson, G. L., et al. (2024). *vegan: Community ecology package* (Version 2.6-x) [R package]. https://CRAN.R-project.org/package=vegan

Parada, A. E., Needham, D. M., & Fuhrman, J. A. (2016). Every base matters: Assessing small subunit rRNA primers for marine microbiomes with mock communities, time series and global field samples. *Environmental Microbiology, 18*(5), 1403-1414. https://doi.org/10.1111/1462-2920.13023

Poulain, A. J., Aris-Brosou, S., Blais, J. M., Brazeau, M., Keller, W., & Paterson, A. M. (2015). Microbial DNA records historical delivery of anthropogenic mercury. *The ISME Journal, 9*(12), 2541-2550. https://doi.org/10.1038/ismej.2015.86

Richard, S., Arnoux, A., Cerdan, P., Reynouard, C., & Horeau, V. (2000). Mercury levels of soils, sediments and fish in French Guiana, South America. *Water, Air, & Soil Pollution, 124*, 221-244.

Scammacca, O., Gunzburger, Y., & Mehdizadeh, R. (2021). Gold mining in French Guiana: Risk assessment at the territorial scale. *The Extractive Industries and Society, 8*(1), 32-43.

Scheelings, T. F., Kodikara, S., Beale, D. J., Van, T. T. H., Moore, R. J., & Skerratt, L. F. (2025). Unravelling the impacts of captivity on saltwater crocodile (*Crocodylus porosus*) cloacal bacterial communities and physiology. *FEMS Microbiology Ecology, 101*, fiaf114. https://doi.org/10.1093/femsec/fiaf114

Smith, S. N., Colston, T. J., & Siler, C. D. (2021). Venomous snakes reveal ecological and phylogenetic factors influencing variation in gut and oral microbiomes. *Frontiers in Microbiology, 12*, 657754. https://doi.org/10.3389/fmicb.2021.657754

Wang, Y., Boyd, E. S., Crane, S., Lu-Irving, P., Krabbenhoft, D., King, S., Dighton, J., Geesey, G., & Barkay, T. (2011). Environmental conditions constrain the distribution and diversity of archaeal *merA* in Yellowstone National Park, Wyoming, USA. *Microbial Ecology, 62*(4), 739-752. https://doi.org/10.1007/s00248-011-9890-z